Available online at www.sciencedirect.com

ScienceDirect

Procedia Engineering 199 (2017) 134–139

Procedia Engineering

www.elsevier.com/locate/procedia

X International Conference on Structural Dynamics, EURODYN 2017

Analysis of dynamic instabilities in bridges under wind action through a simple friction-based mechanical model

De Domenico D.[a], Failla I.[a,*], Ricciardi G.[a]

[a]*Department of Engineering, University of Messina, Villaggio S. Agata, 98166 Messina, Italy*

Abstract

In the field of stability of structures under nonconservative loads, the concept of follower force has long been debated by scientists due to the lack of actual experimental evidence. Bigoni and Noselli's work [2] aimed to investigate flutter and divergence instability phenomena through a purely mechanical model with Coulomb friction represents a praiseworthy attempt to shed light on this issue. A two-degree-of-freedom (DOF) system, conceived as a variant of the Ziegler column, was set up experimentally. The follower load was induced by a frictional force acting on a wheel mounted at the column end, so that the rolling friction vanishes and the sliding frictional force keeps always coaxial to the column, thus representing a tangential follower force. Along this research line, in this contribution a model is elaborated that stems from the analysis of an elastically supported rigid plate that represents the behaviour of a bridge deck suspended on springs and subjected to a wind-induced force. The wind force has been simulated by a Coulomb friction force acting on a wheel mounted on the plate aerodynamic centre, so that the sliding friction force keeps perpendicular to the plate axis throughout the system motion, thus representing a follower force. To properly reproduce the wind force, the friction force is applied to the wheel by a lever mechanism wherein one of the two lever arms involves the plate rotation via a particular circular guide. The corresponding equations of motion of the bridge deck are derived in a completely dimensionless form. Depending on the mechanical characteristics of the plate and the magnitude of the friction force, stability, flutter or divergence phenomena may occur. The occurrence of these phenomena is numerically investigated by integration of the equations of motion. The development of an experimental framework of the model to corroborate these intuitions is the object of an ongoing research.

Peer-review under responsibility of the organizing committee of EURODYN 2017.

Keywords: Flutter instability; divergence instability; follower force; Coulomb friction.

1. Introduction

In the field of stability of structures under nonconservative loads, the concept of *follower force* has long been debated by scientists, and the lack of actual experimental evidence has given rise to a controversy about the real existence of such follower force [1]. By this term we denote a force that is not derivable from a potential and which depends on the instantaneous position of the system, i.e., a configuration-dependent force. The water jet observed at the nozzle of a fluid-conveying pipe or the rocket thrust of a flexible missile are just a few real-world examples of follower forces. Other physical phenomena involving follower forces are related to the so-called "aeroelastic flutter", i.e., the

* Corresponding author. Tel.: +39-0903977167.
E-mail address: ifailla@unime.it

1877-7058
Peer-review under responsibility of the organizing committee of EURODYN 2017.
10.1016/j.proeng.2017.09.195

dynamic instability that may occur in bridges when self-excited oscillations driven by wind increase in amplitude as if the system had an effective negative damping. Many scientists and researchers believe such aeroelastic fluttering triggered the never-before-seen twisting mode of vibration of the Tacoma Bridge in 1940, led to an exponentially growing response and eventually caused the well-known catastrophic collapse of the bridge.

Investigating follower forces from a numerical and, above all, an experimental point of view is rather intricate as they involve either complex fluid-structure interactions or extremely-short-duration effects. Bigoni and Noselli's work [2] aimed to investigate flutter and divergence phenomena through a purely mechanical model with Coulomb friction represents a praiseworthy attempt to shed light on this issue. They demonstrated, by a two-DOF system designed as a variant of the Ziegler column, the existence of the follower force on an experimental basis.

Along this research line, in this contribution a mechanical model is elaborated that stems from the analysis of a horizontal elastically supported rigid plate under aerodynamic forces [3]. This schematic model aims at reproducing the behaviour of a bridge deck suspended on springs and subjected to a wind-induced force. The effects of the wind (follower) forces are simulated by a Coulomb-type friction force. Indeed, we introduce a wheel mounted on a point identifying the aerodynamic centre of the bridge and having axis perpendicular to the longitudinal direction, so that the rolling friction cancels out and the sliding friction force keeps perpendicular to the plate axis throughout the system motion. The friction force accordingly represents a follower force for the system. Similar to the experiment in [2], the vertical reaction entering the Coulomb friction law is applied to the wheel by a lever mechanism. The equations of motion of this simple two-DOF system representing the bridge deck are derived and expressed in a completely dimensionless form. Depending on the magnitude of the friction force and the mechanical characteristics of the plate, stability, flutter or divergence phenomena are observed in the model (which reflects the bridge behaviour for increasing value of the associated wind velocity). The development of an experimental framework of the model to corroborate these intuitions is the object of an ongoing research.

2. Bridge aerodynamics, associated mechanical model and governing equations

The description of the mechanical behaviour of bridges under wind action is a challenging field that has attracted a plethora of researchers [4]. Strictly speaking, highly fluctuating pressure fields arise from the turbulent nature of wind flow, thus resulting in a so-called "aerodynamic load". Additionally, the bridge oscillates according to its vibrational natural characteristics, which gives rise to "aeroelastic" phenomena involving complex fluid-structure interaction. Consequently, resonance-type or instability phenomena may occur depending on the geometry and mechanical properties of the bridge, as well as the main features of the turbulent flow such as its mean velocity.

The above complex phenomena are here simplified in order to investigate the main qualitative aspects of the problem. Let us consider a bridge of length L sketched by a rigid plate (representing the section of the roadway) of unit width and specific mass m per unit length, suspended on springs of stiffness k_1 and k_2 (the stiffness coefficients depend on the actual bridge suspension cables). The system has two DOFs: the rotation θ about the z-axis (i.e., the counterclockwise angle between the horizontal plane and the bridge section in the deformed state), which is depicted as a red arrow in the 3D isometric view, and the vertical motion w of the plate midpoint (or centre of gravity) G. The plate is loaded by wind of velocity v. Under the simplifying hypothesis of slow steady oscillations, as those of very long span suspended bridges, the fluid-structure interaction may be neglected and the wind action can be represented by the wind force resultant $P_w = kv^2 \sin\theta$ acting on the so-called aerodynamic centre of the bridge C, where k is a constant and the location of C does not depend on the angle θ. For two-dimensional incompressible flow C is located at a distance $a = L/4$ relative to the centre of gravity G, on the windward side.

The simplified aerodynamic problem of the bridge discussed above can be reproduced by the schematic mechanical model sketched in Fig. 1: the wind action is replaced by a Coulomb-type friction force exerted by a perfect (massless and fully free of rotating) wheel. The wheel, rigidly connected to the plate of length L identifying the bridge cross-section, slides with pure Coulomb friction on an underlying rigid plane. This plane is ideally touched at a specific point, the aforementioned aerodynamic centre C, and is moved at the speed $-v_p\mathbf{e}_1$, with $\mathbf{e}_1$ indicating the unit vector corresponding to the horizontal direction. For convenience, in Fig. 1 besides the fixed reference system $\mathbf{e}_1 - \mathbf{e}_2$ we introduce a moving system $\mathbf{e}_r - \mathbf{e}_s$. The wheel axis is perpendicular to the longitudinal direction, i.e., it is directed along $\mathbf{e}_s$ (with $\mathbf{e}_s = -\sin\theta\,\mathbf{e}_1 + \cos\theta\,\mathbf{e}_2$), therefore the rolling friction (along $\mathbf{e}_r$) cancels out and the sliding friction force keeps perpendicular to the plate axis throughout the system motion. Consequently, the resulting sliding friction

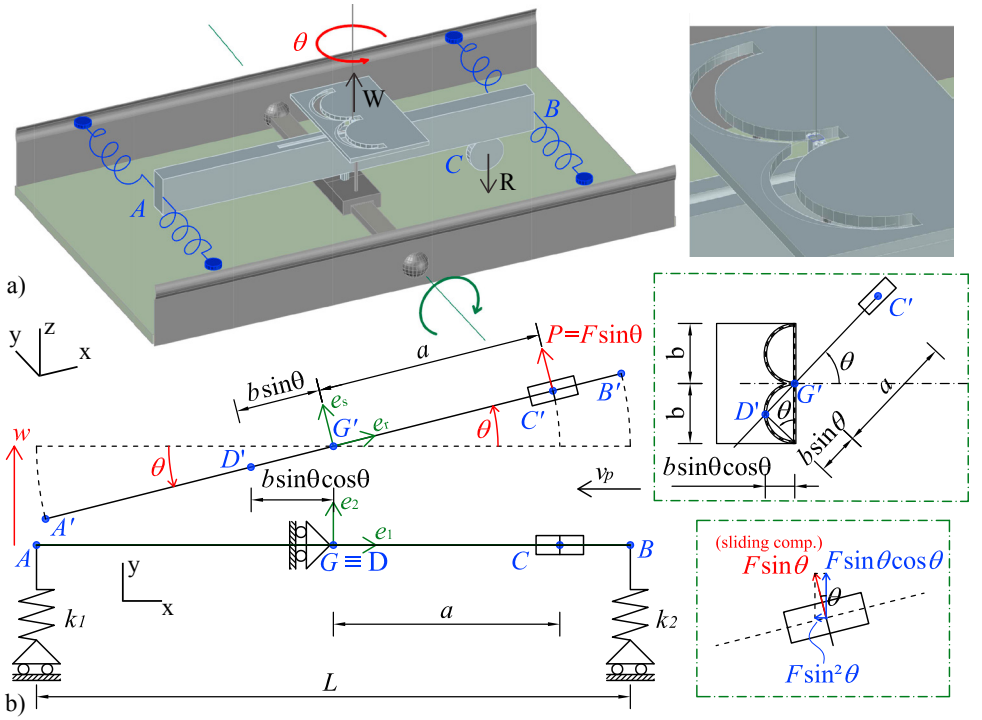

Fig. 1. Friction-based mechanical model outlining the behaviour of a bridge under wind action: a) 3D isometric view; b) 2D sketch of the model

force is a configuration-dependent *follower force* for the system being analysed. The sliding friction force is generated via a lever mechanism using the structure itself as a lever (exploiting the rotation about the y-axis, which is depicted as a green arrow in the 3D isometric view) and applying a dead load W to a point D as sketched in Fig. 1. The originated sliding friction force on the point C is accordingly expressed by the Coulomb friction law in terms of the vertical reaction R. In order for such sliding friction force to properly reproduce the above wind force resultant P_w (in which the $\sin\theta$ term appears), the vertical reaction R should include the angle of rotation θ. To this aim, a specific circular guide with diameter b is designed such that one of the two lever arms involves the sought $\sin\theta$ term, so that

$$P = R\mu(\dot{C}_p^s) = W\,\frac{b\,\sin\theta}{a}\mu\,(\dot{C}_p^s) = F\,\sin\theta, \quad \text{with } \mu\,(\dot{C}_p^s) = \begin{cases} \mu\,\mathrm{sgn}\left(\dot{C}_p^s\right) & \text{if } \dot{C}_p^s \notin [-\varepsilon,\varepsilon] \\ \mu\left(2-\frac{|\dot{C}_p^s|}{\varepsilon}\right)\frac{\dot{C}_p^s}{\varepsilon} & \text{if } \dot{C}_p^s \in [-\varepsilon,\varepsilon] \end{cases} \tag{1}$$

where a superimposed dot denotes the derivative with respect to time, $F = (b/a)\,W\mu\,(\dot{C}_p^s)$ and $\mu(\dot{C}_p^s)$ is the friction coefficient. In other words, D is forced to follow the circular guide. In Eq. (1) the Coulomb friction law has been simplified as no stiction is considered (which would lead to introducing different static and dynamic μ values) and the regularization proposed in [5] is adopted, with ε being a small parameter, say $\varepsilon = 10^{-5}$ m/s. Considering the displacement vector $\mathbf{C'C} = (a\cos\theta - a)\,\mathbf{e}_1 + (w + a\sin\theta)\,\mathbf{e}_2$, the velocity of the contact point C is $\dot{\mathbf{C}} = (-a\,\dot\theta\sin\theta)\,\mathbf{e}_1 + (\dot w + a\,\dot\theta\cos\theta)\,\mathbf{e}_2$. From Eq. (1) the friction coefficient μ is a function of the velocity $\dot{C}_p^s$, i.e., the sliding component of the velocity of the wheel relative to the plane $\dot{\mathbf{C}}_p = \dot{\mathbf{C}} - \mathbf{v}_p = \dot{\mathbf{C}} + v_p\mathbf{e}_1$ projected along $\mathbf{e}_s$, which is expressed as follows

$$\dot{C}_p^s = \dot{\mathbf{C}}_p \cdot \mathbf{e}_s = (\dot{\mathbf{C}} + v_p\mathbf{e}_1)\cdot\mathbf{e}_s = a\,\dot\theta\sin^2\theta - v_p\sin\theta + \dot w\cos\theta + a\,\dot\theta\cos^2\theta = a\,\dot\theta - v_p\sin\theta + \dot w\cos\theta. \tag{2}$$

According to D'Alembert's principle, the equations of motion, obtained as the equations of dynamic equilibrium of vertical forces and moments about the centre of the plate G , read

$$\begin{aligned} &mL\ddot w + \beta_t\dot w + (k_1+k_2)w + (k_2-k_1)\frac{L}{2}\sin\theta = F\,sin\theta\cos\theta \\ &\frac{mL^3}{12}\ddot\theta + \beta_r\,\dot\theta + (k_2-k_1)w\frac{L}{2}\cos\theta + (k_1+k_2)\frac{L^2}{4}\sin\theta\cos\theta = F\,\sin\theta\,a \end{aligned} \tag{3}$$

where for the sake of generality, Voigt-type (viscous) translational and rotational damping is considered, whose corresponding coefficients are indicated as β_t and β_r, respectively. Both the forms of damping are assumed as being concentrated at the midpoint G wherein a linear guide allowing the vertical motion w and a spherical hinge allowing the rotation θ are placed. The set of two coupled nonlinear differential equations (3) describes both the mechanical model under frictional forces of Fig. 1 and the bridge model under aerodynamic forces. Stability analysis of Eqs. (3) will accordingly indicate whether stability, flutter or divergence phenomena occur in the bridge. For the sake of convenience, the set of equations (3) is rewritten in a completely dimensionless form. To this aim, we introduce the following positions and auxiliary variables

$$u = \frac{w}{L}\,[-];\quad \alpha = \frac{a}{L}\,[-];\quad \frac{k_1}{mL} = \omega^2\,[T^{-2}];\quad \frac{k_2}{k_1} = \chi\,[-];\quad \frac{\beta_t}{\omega\, mL} = \xi_t\,[-];\quad \frac{\beta_r}{\omega\, mL^3} = \xi_r[-];\quad f = \frac{F}{mL^2\omega^2}[-]. \tag{4}$$

Additionally, a dimensionless time variable $\tau = \omega\, t$ is introduced so that the first and second derivatives are given by $\dot{x} = \partial x/\partial t = \omega^2\, \partial x/\partial \tau = \omega^2 x'$ and $\ddot{x} = \partial^2 x/\partial t^2 = \omega^2\, \partial^2 x/\partial \tau^2 = \omega^2 x''$ (with $x = u, \theta$). We eventually get

$$\begin{aligned} &u'' + \xi_t\, u' + (1+\chi)u + (\chi - 1)\frac{1}{2}\sin\theta = f sin\theta\cos\theta \\ &\theta'' + 12\,\xi_r\,\theta' + 6\,(\chi - 1)u\cos\theta + 3\,(1+\chi)\sin\theta\cos\theta = 12\, f\,\sin\theta\,\alpha \end{aligned} \tag{5}$$

that is the sought system of differential equations in terms of the dimensionless variables $u = u(\tau)$ and $\theta = \theta(\tau)$.

3. Stability analysis of Eqs. (5): flutter and divergence phenomena

Due to the large-displacement assumption, Eqs. (5) are two *nonlinear* differential equations. Stability analysis of the model is performed with regard to the linearized counterpart of Eqs. (5) by a Taylor series expansion, in the form

$$\begin{aligned} &u'' + \xi_t\, u' + (1+\chi)\, u + (\chi - 1)\frac{1}{2}\theta = f\,\theta \\ &\theta'' + 12\,\xi_r\,\theta' + 6\,(\chi - 1)\, u + 3\,(1+\chi)\,\theta = 12\, f\,\theta\,\alpha \end{aligned} \tag{6}$$

that is the system governing the dynamics of the model for configurations in a small neighbourhood of the trivial one ($u = \theta = 0$), i.e., under the small-displacement assumption ($\sin\theta \to \theta, \cos\theta \to 1$). The loss of stability due to divergence (equivalent to static buckling) may be determined by setting $u'' = \theta'' = 0$ and $u' = \theta' = 0$. Consequently, Eqs. (6) become a system of two linear algebraic homogeneous equations and the loss of stability occurs when $\det[c_{ij}] = 0$ with c_{ij} being the coefficients of u and θ, which yields

$$f_{\rm cr} = \frac{2\chi}{1 - \chi + 2\alpha(1+\chi)} \tag{7}$$

from which it is found that divergence is possible only if $\chi < (2\alpha + 1)/(1 - 2\alpha)$ (for $\alpha = 1/4$, $\chi < 3$). In reality, divergence may also occur for a smaller value than that reported in (7) as will be demonstrated below. Indeed, the critical loads for flutter and divergence are actually computed by substituting two trial time-harmonic functions $u = Ue^{-i\omega\tau}$ and $\theta = \Theta e^{-i\omega\tau}$ into Eqs. (6) and investigating the resulting dynamic solutions. Two linear algebraic homogeneous equations for the amplitudes U and Θ arise, whereby non-trivial solutions are possible only if the determinant of the coefficient matrix vanishes, which yields the following fourth-order characteristic equation

$$\omega^4 + p_1\omega^3 + p_2\omega^2 + p_3\omega + p_4 = 0 \tag{8}$$

where the coefficients are

$$\begin{aligned} &p_1 = 12\, i\,\xi_r + i\,\xi_t; \quad p_2 = 4\,(3f\alpha - 3\xi_r\xi_t - \chi - 1); \\ &p_3 = -3\, i\,\left(4\xi_r(1+\chi) + \xi_t(1 - 4f\alpha + \chi)\right); \quad p_4 = 6\,(2\chi - f\,(1 - \chi + 2\alpha(1+\chi))). \end{aligned} \tag{9}$$

In the absence of viscosity, the p_2 coefficient does not include damping terms, p_1 and p_3 vanish so that Eq. (8) turns out to be a second-order equation in ω^2 whose solutions are $2\omega_i^2 = -p_2 \pm \Delta^{1/2}$ with $\Delta = p_2^2 - 4p_4$. This gives rise to the following possibilities: 1) for $p_2 < 0$ and $\Delta > 0$ four real ω_i values arise, a situation corresponding to stability as

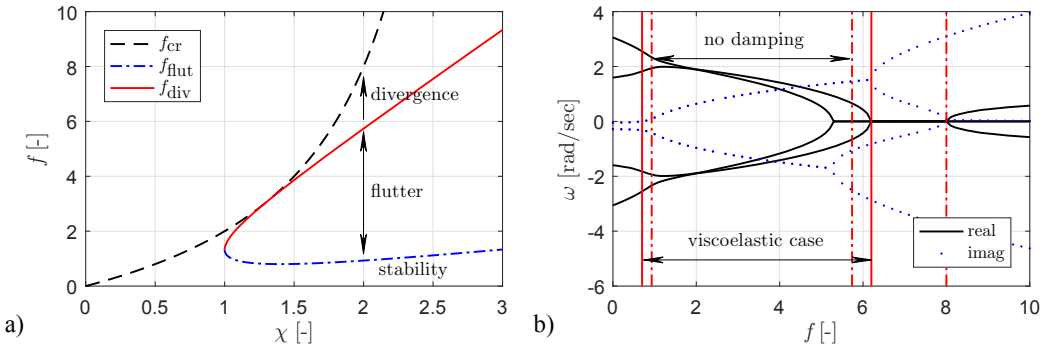

Fig. 2. Stability analysis of Eqs. (6): a) critical load dependence on χ; b) real and imaginary parts of the frequencies from Eq. (8) for $\chi = 2$

the vibrations are sinusoidal with constant amplitude; 2) for $\Delta < 0$ there are two complex-conjugate pairs of ω_i, which indicates flutter instability as the solutions are sinusoidal with exponentially varying amplitude, two blowing-up and two decaying with time; 3) for $p_2 > 0$ and $\Delta > 0$ two purely imaginary complex-conjugate pairs of ω_i arise, which denotes divergence instability as the vibrations are of exponential-type, two amplifying and two decaying with time. As a subcase of 3), if $p_2 > 0$ and $p_4 = 0$ two frequencies are purely imaginary and the other two are zero (since $\Delta^{1/2} \equiv p_2$), all denoting divergence. The latter situation ($\omega = 0$) has already been discussed in (7) since $p_4 = 0$, considering Eq. (9), corresponds to $f = f_{cr}$ reported in Eq. (7). It is worth noting that the actual critical load for divergence is computed by setting $\Delta = 0$ with $p_2 > 0$, which leads to a smaller load than that reported in (7) by setting $p_4 = 0$. On the other hand, the critical load for flutter is given by $\Delta = 0$ with $p_2 < 0$. For example, for $\alpha = 1/4$ the following critical load for flutter and divergence are obtained, respectively

$$f_{\text{flut}} = \frac{2}{3}\left(-1 + 3\chi - \sqrt{5\chi^2 - 2\chi - 3}\right), \quad f_{\text{div}} = \frac{2}{3}\left(-1 + 3\chi + \sqrt{5\chi^2 - 2\chi - 3}\right) \tag{10}$$

from which it is found that flutter occurs only if $\chi > 1$. Finally, for $p_4 < 0$, i.e., for $f > f_{cr}$, the discriminant Δ is always positive, two frequencies are real and two are purely imaginary complex-conjugate, denoting divergence.

When the damping terms are included, the four characteristic frequencies resulting from Eq. (8)) give rise to the following possibilities: 1) $\text{Im}(\omega_i) < 0$ means stability; 2) $\text{Im}(\omega_i) > 0$ and $\text{Re}(\omega_i) \neq 0$ corresponds to flutter instability; 3) $\text{Im}(\omega_i) > 0$ and $\text{Re}(\omega_i) = 0$ leads to divergence instability. In Fig. 2 the above concepts are clarified: in Fig. 2a) the three critical loads of Eqs. (7)) and $(10)_{1,2}$ are depicted for $\alpha = 1/4$, from which we notice than $f_{\text{div}} < f_{cr}$ throughout the range of χ of interest. Furthermore, as seen above flutter may occur only if $\chi > 1$, whereas for $0 < \chi \leq 1$ increasing the load f would lead to a sharp transition from stability to divergence instability. Generally, the two cables of a suspended bridge have approximately the same stiffness, i.e., $\chi \approx 1$. In order to highlight a wide flutter range in the present stability analysis, in Fig. 2b) the solution frequencies of the characteristic equation (8) are reported for a quite exaggerated stiffness ratio $\chi = 2$: the real and imaginary parts of ω_i are plotted separately in order to identify the associated stability behavior. We compare the regions of flutter ($\text{Im}(\omega_i) > 0$ and $\text{Re}(\omega_i) \neq 0$) in the viscoelastic case for some arbitrary damping ratios ($\xi_t = \xi_r = 0.05$), $f_{\text{flut}} = 0.7$, $f_{\text{div}} = 6.2$ (continuous lines in Fig. 2b)), and in the absence of damping ($\xi_t = \xi_r = 0$), $f_{\text{flut}} = 0.93$, $f_{\text{div}} = 5.74$ (dash-dotted lines in Fig. 2b)): this comparison demonstrates that the viscosity slightly broadens the interval of flutter as compared to the non-damped case.

4. Dynamic solutions by integration of the nonlinear equations of motion

The stability analysis discussed in the previous Section is further investigated by examining the dynamic solutions of Eqs. (5). Depending on the load magnitudes, stability, flutter and divergence phenomena are expected to occur. For the same mechanical parameters as in Fig. 2b) ($\chi = 2$, $\alpha = 1/4$, $\xi_t = \xi_r = 0.05$), three increasing load magnitudes are analyzed, namely $f = 0.2$, 1 and 7, which correspond to stability, flutter and divergence instability, respectively. The resulting time-histories of the response in terms of u and θ are reported in Fig. 3. According to the expectations, stability is characterized by a decaying response with time (due to damping), flutter instability becomes manifest by

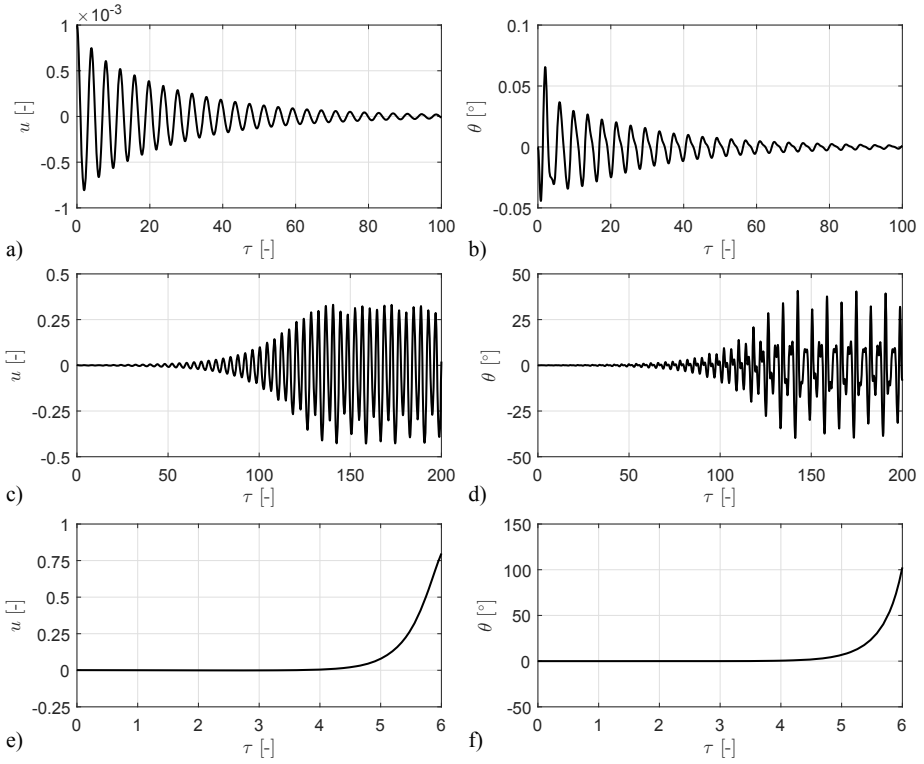

Fig. 3. Dynamic solution of Eqs. (5): a), b) stability; c), d) flutter instability; e), f) divergence instability

a blowing-up vibrational response that eventually attains a steady state (in line with the experimental findings in [2]), and divergence instability is an exponentially growing motion without oscillations.

5. Concluding remarks and future developments

In this contribution, the occurrence of dynamic instabilities in bridges under wind action has been numerically investigated. Following an experimental work of the literature [2], the stability behaviour of the bridge has been analysed via a mechanical model in which the aerodynamic (wind) forces have been simulated by a Coulomb-type friction force. A two-DOF mechanical model has been designed in which the friction force has been applied by means of a wheel and represents a follower force for the system being analysed. After discussing the main assumptions of the model, the equations of motion have been derived and the stability analysis has been performed so as to identify the flutter and divergence regions depending on the mechanical parameters of the system and the magnitude of the friction force. Stability, flutter and divergence instability have been scrutinized by integrating the nonlinear equations of motion. The numerical investigation carried out in this study represents the basis for the development of an experimental framework of the model, which is the object of an ongoing research.

References

[1] I. Elishakoff, Controversy associated with so-called “follower force”: critical overview, Appl. Mech. Rev. 58 (2005) 117-142.
[2] D. Bigoni, G. Noselli, Experimental evidence of flutter and divergence instabilities induced by dry friction, Journal of the Mechanics and Physics of Solids, 59 (2011), 2208-2226.
[3] Z.P. Bazant, L. Cedolin, Stability of Structures, Elastic Inelastic, Fracture and Damage Theories, World Scientific, Singapore, (2010).
[4] C. Borri, C. Costa, Bridge Aerodynamics and Aeroelastic Phenomena, in: T. Stathopoulos (ed.), Wind Effects on Buildings and Design of Wind-Sensitive Structures, CISM Courses and Lectures No. 493, Springer Wien New York, 2007, pp. 167-200.
[5] [5] J.T. Oden, J.A.C. Martins, Models and computational methods for dynamic friction phenomena, Comput. Meth. Appl. Mech. Eng. 52 (1985) 527-634.